J. Am. Soc. Mass Spectrom. (2013) 24:1493–1500
DOI: 10.1007/s13361-013-0704-z

RESEARCH ARTICLE

Quadrupole Mass Filter: Design and Performance for Operation in Stability Zone 3

Sarfaraz U. A. H. Syed, Thomas J. Hogan, Mariya J. Antony Joseph, Simon Maher, Stephen Taylor

Department of Electrical Engineering and Electronics, University of Liverpool, Liverpool, L69 3GJ, UK

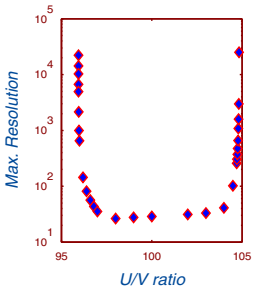

Abstract. The predicted performance of a quadrupole mass filter (QMF) operating in Mathieu stability zone 3 is described in detail using computer simulations. The investigation considers the factors that limit the ultimate maximum resolution (R_{max}) and percentage transmission (%Tx), which can be obtained for a given QMF for a particular scan line of operation. The performance curve (i.e., the resolution (R) versus number (N) of radio frequency (rf) cycles experienced by the ions in the mass filter) has been modeled for the upper and lower tip of stability zone 3. The saturation behavior of the performance curve observed in practice for zone 3 is explained. Furthermore, new design equations are presented by examining the intersection of the scan line with stability zone 3. Resolution versus transmission characteristics of stability zones 1 and 3 are compared and the dependence of performance for zones 1 and 3 is related to particular instrument operating parameters.

Key words: Quadrupole mass filter (QMF), Resolution, U/V ratio, Number of rf cycles, Performance curve, Transmission, Stability zone 3

Received: 23 March 2013/Revised: 31 May 2013/Accepted: 3 June 2013/Published online: 18 August 2013

Introduction

The use of a quadrupole field for mass spectrometry (MS) dates back to the pioneering work of Wolfgang Paul and co-workers in the 1950s [1], and is widely used as a mass filter in a quadrupole mass spectrometer (QMS), an ion guide or a linear ion trap [2]. Decades later, QMSs have flourished in both industry and research with applications ranging from analysis of simple residual gas mixtures to that of complex organic materials. All these form an imposing testimony to the value of this instrument [3, 4]. The characteristics that have ensured its widespread use include versatility, low-cost, accuracy, and mass range. There are a number of applications that require high resolution. Example applications include the quantitative measurement of hydrogen isotopes in the presence of helium isotopes that generally requires a minimum resolution of 930 [4–7], and the quantitative measurement of carbon monoxide in the presence of nitrogen that requires a minimum resolution of 2500 for mass discrimination [8]. These resolutions, especially at the lower end of the mass range (1–6 u) are not readily achievable with commercially available QMS instruments.

Correspondence to: Stephen Taylor; *e-mail:* s.taylor@liv.ac.uk

Most commercial QMS instruments operate in stability zone 1. However, there are certain advantages, such as mass spectral peak shape, reduction of low mass tailing, and increased resolution, to be obtained if the QMS is operated in the third stability zone. It has previously been demonstrated that QMS operation in stability zone 3 can provide the required resolution to separate low mass isotopes [4–7], and carbon monoxide from nitrogen [8]. Operation in stability zone 3 requires higher operating voltages, which have previously been seen as a disadvantage. Nevertheless, with the introduction of miniature QMFs, the increased voltage budget may not be considered as an economic obstacle anymore [9]. Comparing stability zone 1, which has a tip at ($a = 0.23699$, $q = 0.706$) on the Mathieu stability diagram, stability zone 3 is a sloping rectangular area providing two tips, one at the upper left tip ($a = 3.16$, $q = 3.23$), and the second at lower right tip ($a = 2.52$, $q = 2.82$) that enable high resolution mass scanning to be achieved [8]. With stability zone 3 the ions require a lower exposure to number of rf cycles to achieve the same resolution compared with zone 1, albeit at the expense of reduced transmission [10]. When the resolution is limited by ion residence time in the QMF, the resolution (R) is known to be dependent on the number (N) of radio frequency (rf) cycles experienced by the ions in the mass filter [11], according to $\mathbf{R} = N^n/K$, where n approximately equal to 2 and K

is a constant that depends on operating conditions. For operation of QMF in stability zone 3, Hiroki et al. performed computer simulations and determined the relationship at the upper tip $\boldsymbol{R = 1.7\,N^2}$ and at the lower tip $\boldsymbol{R = 0.69\,N^2}$ [5]. The same simulations showed $\boldsymbol{R = N^2/10.9}$ for the stability zone 1, which is in reasonable agreement with the calculation of Paul et al. [12]. Titov found $\boldsymbol{R = 1.7\,N^2}$ and Du et al. measured at 50 % peak width definition as $\boldsymbol{R = 1.4\,N^2}$ [13]. Konenkov and Kratenko experimentally found $\boldsymbol{R = 0.7\,N^2}$ [14]. They also found that with increasing N^2, the resolution approached a constant saturation level. This was thought to be a consequence of poor coupling between the ion source and the analyzer, and low quadrupole field quality producing increased amplitude of ion oscillations with increasing R.

In our previous work [15], we have shown that the saturation behavior observed in practice for QMF operating in stability zone 1 [11, Chapter 6] with increasing N is seen to be a feature of the QMF and, therefore, not necessarily due to mechanical deficiencies in QMF manufacture. The saturation region of the performance curve for QMF operation in zone 1 can be modeled according to $\boldsymbol{R = q(1 - 2c^N)/\Delta q}$, where c is a constant and Δq is the width of the intersection of the operating scan line with the stability zone, measured at q-axis of the Mathieu stability diagram. Also, for stability zone 1 it was shown that the ultimate maximum resolution (R_{max}) for a particular value of scan line can be related to percentage direct current (DC) voltage (U) to rf voltage (V) ratio as: $\boldsymbol{R_{max} = q/(0.9330\text{-}0.00933U/V)}$. This paper, therefore, extends the previous work and investigates the performance characteristics for a QMF operating in stability zone 3. We present new design equations in terms of maximum obtainable resolution $\boldsymbol{R_{max}}$, U/V ratio, and stability parameters *(a, q)*. Also, in this work the resolution versus transmission characteristics of stability zone 3 were studied in detail, leading to some novel conclusions.

Theory

The theory for ion motion in a QMS is well documented in the scientific literature [15, 16], and is reproduced here for completeness. A QMF consisting of a parallel array of four electrodes mounted in square configuration produces a central electric field whose strength increases linearly with increasing displacement from the central axis and is independent in x and y (ideal quadrupole field). When driven by the correct combination of DC and rf voltages, the electrode assembly is capable of providing mass filtering action. With the voltages defined in Equations (1) and (2), the behavior of the ions as they pass through the QMF can be defined by the Mathieu Equation (3) [16].

$$\phi_x = (U - V\cos\omega t) \tag{1}$$

$$\phi_y = -(U - V\cos\omega t) \tag{2}$$

$$\frac{d^2u}{d\xi^2} + (a_u - 2q_u cos(2\xi))u = 0 \tag{3}$$

Where $u = x$ or y and

$$a_u = a_x = -a_y = \left(\frac{8eU}{mr_0^2\omega^2}\right) \tag{4}$$

$$q_u = q_x = -q_y = \left(\frac{-4eV}{mr_0^2\omega^2}\right) \tag{5}$$

where V is the zero-to-peak amplitude of rf voltage oscillating with angular frequency ω (expressed in radians per s), U is the applied DC voltage, t is the time, e is the charge on the ion, and m is the ion's mass. Under normal operating conditions, the mass filtering action of the QMF is controlled by electrode voltages U and V. The ratio of the voltages U and V controls the QMF resolution setting and the voltage V sets the mass scale. The mass scan line shows the a and q values of ions of different mass to charge ratios for a given DC and rf voltage ratio. QMF resolution was found to be dependent on number of rf cycles (N) experienced by the ions in the mass filter. N may be calculated by: $\boldsymbol{N = (f\,l)/\sqrt{(2E_z/m)}}$ where l is the length of the mass filter, f is frequency of the rf voltage, and E_z the ion energy. From the mass spectrum obtained by the numerical simulation, the resolution R can be calculated by using the equation $R = M/\Delta M$, where M is the mass of the given spectral peak and ΔM is the width of the mass peak measured at 10 % of its height [11], unless otherwise stated.

Computer Models Used

QMS2-Hyperbolic

A custom software program (QMS2-hyperbolic) developed in Visual C++ environment described previously [15] is used in this work. The program calculates ion trajectories by solving the Mathieu equations using a fourth order Runge–Kutta algorithm. Mass scans are computed by ramping the values of U and V with fixed U/V ratio passing through the origin, which sets the resolution of an instrument.

A second program (IonSrc) allows entry conditions for large number of ions (typically 10^8) to be specified, which are supplied to the mass filter calculation engine to simulate individual trajectories in each case. The IonSrc program assumes a uniformly illuminated ion distribution across a user-defined ion source exit radius. Each ion is injected into the QMF with random phase with respect to the rf at the time of entry. Finally, Matlab and OriginPro 8.5 are used to

post-process the data and for the generation of graphical results.

Simulation Method

All the simulations use 200 steps across the mass range with 5×10^5 ions injected and traced at each mass step. Mass peaks for $^{40}Ar^+$ are generated for a hyperbolic quadrupole mass filter with inscribed radius (field radius) of 1.5 mm. The frequency of the rf voltage used in the simulation was 4 MHz and the input ion energy (E_z) was chosen as $5eV$. The ion source radius (r_{ie}) was selected as 0.5 mm. The length of the mass filter was varied in order to vary the number of rf cycles the ion experiences. It is assumed in the model that the QMF control setting U/V = 100 % corresponds to the U/V ratio at q = 3.0 and a = 2.8, which is near the center of the stability zone 3, the middle region (MR) of the stability zone. With increasing U/V ratio the scan line approaches the upper left tip of stability zone 3 (a = *3.16*, q = *3.23*) i.e., the upper tip region (UTR), whereas, with decreasing U/V ratio the scan line approaches the lower right tip of stability zone 3 (a = *2.52*, q = *2.82*) i.e., the lower tip region (LTR). A U/V of 104.8311 % corresponds to the upper left tip of zone 3, whereas a U/V of 95.94243 % corresponds to the lower right tip of zone 3. These three areas of operation in stability zone 3 are illustrated in Figure 1a. For zone 1 operation, U/V = 100 % corresponds to q = 0.70600, a = 0.23699. In the simulations account of fringing fields at the entrance or exit of the mass filter has not been considered, and the initial velocities in the x and y directions are zero. Also, the simulations using QMS2 hyperbolic are for the case of an ideal (but finite length and finite field radius) quadrupole field with zero mechanical misalignments.

Results and Discussion

Performance of a QMF Operating in Stability Zone 3

Figure 1b shows the dependence of resolution measured at 10 % peak width definition, on the number of rf cycles at three different U/V ratios 104.81 %, 104.82 %, and 104.83 % for the UTR of stability zone 3. It can be seen from Figure 1b that as the number of rf cycles increases, resolution increases with a finite slope and then the curve showing the dependence starts to saturate. The values of n and K for the linear region of the performance curve for U/V ratio 104.83 % are 2.14 and 10.3, for U/V ratio 104.82 % are 2.17 and 4.22, and for U/V 104.81 % are 1.56 and 0.43, respectively. These values are in agreement with those obtained experimentally by Konenkov and Kratenko [14]. Figure 1c shows the dependence of resolution on number of rf cycles at three different U/V ratios 95.946 %, 95.945 % and 95.944 % for the LTR of stability zone 3.

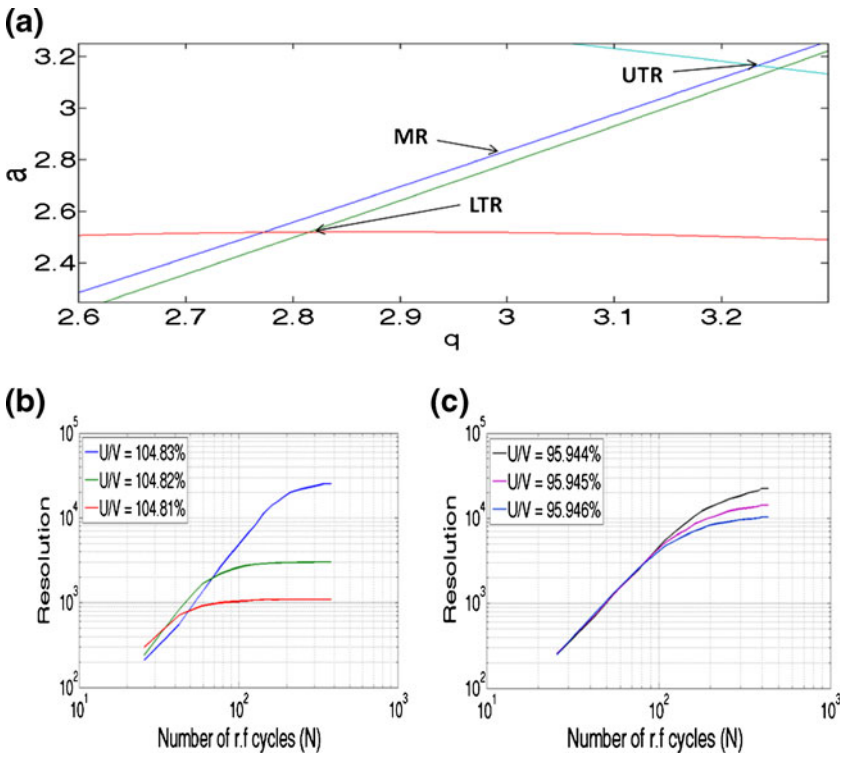

Figure 1. **(a)** Details of stability zone 3; **(b)** the dependence of resolution on the number of rf cycles for QMF operation at the upper tip region (UTR) of stability zone 3 at different U/V ratios predicted by QMS2-hyperbolic; **(c)** the dependence of resolution on the number of rf cycles for QMF operation at the lower tip region (LTR) of stability zone 3 at different U/V ratios predicted by QMS2-hyperbolic

Similarly, as the case with UTR resolution increases and then it saturates. The values of n and K for the linear region of the performance curve for U/V ratio 95.946 % are 2.04 and 2.81, for U/V ratio 95.945 % are 2.09 and 3.41, and for U/V ratio 95.944 % are 2.14 and 4.20 respectively.

Using QMS-2 hyperbolic, experimentally observed saturation behavior of the performance curve for QMF operating in the UTR by Konenkov and Kratenlo [14] shown in Figure 2a and by Du et al. [10] shown in Figure 2c, has been simulated and reproduced as Figure 2b and d. Comparing Figure 2a with Figure 2b, and Figure 2c with Figure 2d, the behavior of the performance curve is similar, resolution (measured at 50 % peak width definition) increases with increasing N^2 and then the curve saturates. As published previously [15], the intersection of the scan line below the tip increases the pass-band and in turn limits the resolution of a QMF to a finite maximum value, which is given by ($R_{max} = q/\Delta q$) for a given mass even if the number of rf cycles are increased by increasing the length or frequency or by decreasing ion energy. The saturation behavior in resolution observed by [10, 14] with increasing N^2 is thus seen to be the feature of the QMF and, therefore, not necessarily due to mechanical deficiencies, such as poor coupling between the ion source and the analyzer and low quadrupole field quality in QMF manufacture. However, mechanical deficiencies can affect the peak shapes e.g., increase in low and/or high mass tailing and loss of transmission, thus decreasing resolution. This is the reason that there is a discrepancy between measured values of resolution and simulated values at certain points of N^2, upon comparison of Figure 2a with Figure 2b, and Figure 2c with Figure 2d, respectively.

The equation $R = N^n/K$ is not valid for the saturation regions of performance curves obtained for the UTR as well as for the LTR. In Figure 3a and b the saturation regions are modelled using OriginPro 8.5. A good representation of the saturation behavior of the performance curve for both UTR and LTR is given by $\boldsymbol{R = a - bc^N}$, where a, b, and c are constants the values of which depend upon the U/V ratio. Figure 3a (UTR, U/V ratio 104.83 %) and Figure 3b (LTR, U/V ratio 95.944 %) show the relationship between N and R obtained using QMS2-hyperbolic (square symbols) and a fitted curve to the data (red line) using OriginPro 8.5. The value of the coefficient of determination (COD) termed as R_c^2 for both the cases was found to be around 0.99, indicating a good regression fit between the curves (R_c^2 of 1 indicates that the regression line perfectly fits the data).

Dependence of Ultimate Maximum Resolution on U/V Ratio for QMF Operating in Stability Zone 3

A program that is a direct conversion of the corresponding Fortran program in Zhang and Jin [17] was used to calculate the details of the Mathieu stability zones. The program generates the boundaries of the stable and unstable areas of the Mathieu stability diagram in a discretized form. These values are then imported into a Matlab program, which plots

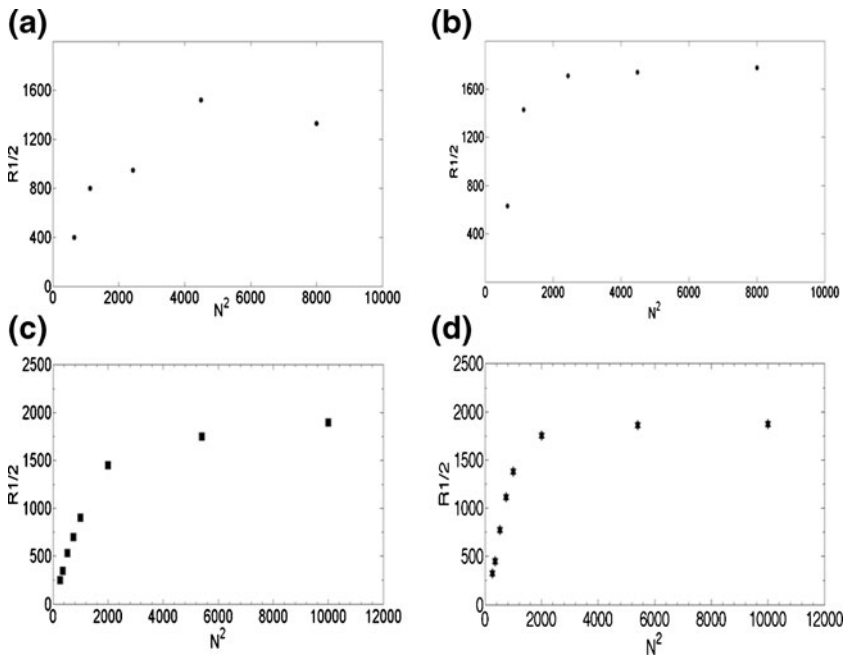

Figure 2. **(a)** The measured resolution at half height *R1/2* for $^{40}Ar+$ *versus* the square of the number of cycles spent in the quadrupole field (N^2) for operation at the UTR of the zone 3, reproduced from [14]; **(b)** the simulated resolution at half height *R*1/2 for $^{40}Ar+$ *versus* the same number of square of the number of cycles (N^2) as Figure 2a using QMS2, U/V = 104.805 %; **(c)** the measured resolution at half height *R1/2* for $^{36}Ar+$ *versus* the square of the number of cycles spent in the quadrupole field (N^2) for operation at the UTR of the zone 3, reproduced from [10]; **(d)** The simulated resolution at half height *R*1/2 for $^{36}Ar+$ *versus* the same number of square of the number of cycles (N^2) as Figure 2c using QMS2, U/V = 104.811 %

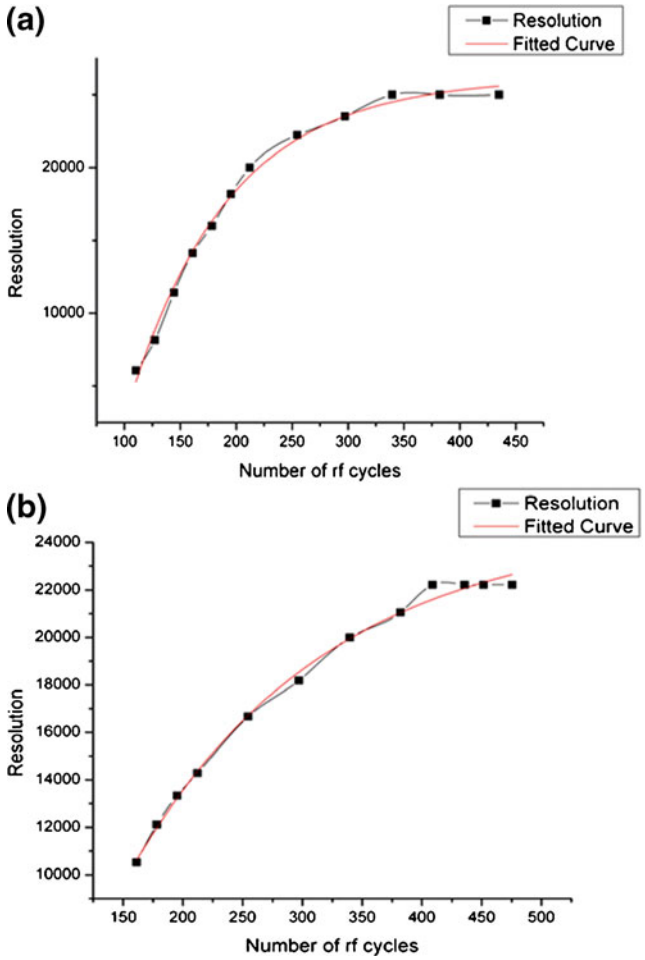

Figure 3. **(a)** The dependence of resolution for $^{40}Ar+$ on number of rf cycles for stability zone 3 (fit obtained using Origin 8.5) at U/V = 104.83 % (UTR); **(b)** the dependence of resolution for $^{40}Ar+$ on number of rf cycles for stability zone 3 (fit obtained using Origin 8.5) at U/V 95.944 % (LTR)

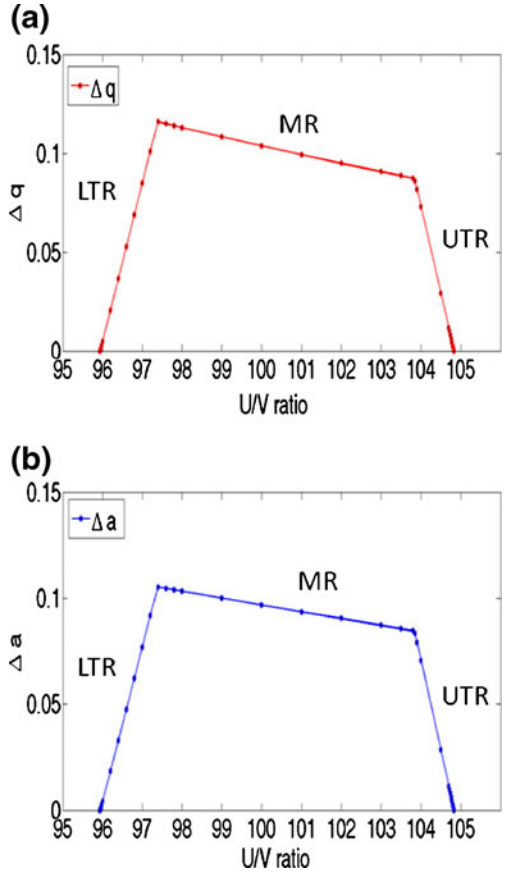

Figure 4. **(a)** Variation of Δq with U/V ratio for stability zone 3; **(b)** variation of Δa with U/V ratio for stability zone 3

the full Mathieu stability diagram. The scan line is then drawn over the Mathieu equation and the points of intersection with the Mathieu stability boundaries can be detected. By altering the active area of the graph and the scan line, different scan line stability zone combinations can be plotted. The reliance of R_{max} on stability parameter $\boldsymbol{a}$ has been investigated in this work, and it is established that R_{max} can be related to $\boldsymbol{a}$ as $\boldsymbol{R_{max} = a/\Delta a}$. Where, Δa is the width of the intersection of the operating scan line with the stability zone, measured at a-axis of the Mathieu stability diagram. Furthermore, the intersection of scan line with stability zone 3 at different U/V ratios have been investigated, and Δq, Δa were carefully calculated.

Figure 4a shows variation of Δq along the whole range of U/V ratios that includes LTR, MR, and UTR for stability zone 3; correspondingly, Figure 4b shows variation of Δa along the whole range of U/V ratios that includes LTR, MR, and UTR. It can be seen from the variation of Δq and Δa with U/V ratio in Figure 4a and b that the three regions (LTR, MR, and UTR) can be divided according to U/V ratios or (a, q). The lower tip region LTR covers U/V ratios from 95.94243 % (corresponds to the lower right tip of zone 3) to 97.4 %. The middle region MR covers U/V ratios from 97.4 % to 103.8 %, whereas, the upper tip region UTR covers U/V ratios from 103.8 % to a U/V of 104.8311 % that corresponds to the upper left tip of stability zone 3. It is evident from Figure 4 that zone 3 has three regions of operation (i.e., LTR, MR, and UTR). A good mathematical relationship between (1) Δq and U/V ratio; (2) Δa and U/V ratio for three different regions is shown in Table 1. In the derived relationships, a high number of significant figures were found to be necessary for maximum accuracy of resolution calculations, particularly when close to the

Table 1. Mathematical Relationship between Δq and U/V Ratio; Δa and U/V Ratio

Region	Δq	Δa
LTR	(−7.68116 + 0.08006009U/V)	(−6.97891 + 0.072740521U/V)
MR	(0.54974 - 0.004460000U/V)	(0.42089 - 0.003240000U/V)
UTR	(9.21060 - 0.087861304U/V)	(8.92643 - 0.085150563U/V)

boundaries of the stability diagram (i.e., at LTR, MR, and UTR).

By substituting the value of Δq in $R_{max} = q/\Delta q$ and Δa in $R_{max} = a/\Delta a$, the following relationships between the maximum resolution R_{max} for a particular scan line (U/V ratio in percentage) have been established. For the Lower tip region LTR R_{max} can be related to U/V ratio as:

$$R_{max} = q/(-7.68116 + 0.080060091U/V), and$$

$$R_{max} = a/(-6.97891 + 0.072740521U/V)$$

For the middle region MR R_{max} can be related to U/V ratio as:

$$R_{max} = q/(0.54974 - 0.004460000U/V), \quad and$$

$$R_{max} = a/(0.42089 - 0.003240000U/V)$$

For the Upper tip region UTR R_{max} can be related to U/V ratio as:

$$R_{max} = q/(9.21060 - 0.087861304U/V), \quad and$$

$$R_{max} = a/(8.92643 - 0.085150563U/V)$$

It should be noted that in the above relationships, the values of a and q are constant in all the equations. Since the program QMS2-hyperbolic considers a U/V of 100 % at the center of stability zone 3, the equations are developed according to q = 3.0 and a = 2.8, which are the values of a and q near the center of stability zone 3. Figure 5a shows comparison of maximum resolution obtained in the simulations and the R_{max} calculated for the ideal case (developed equations) using the Mathieu stability diagram at different U/V ratios for LTR (95.94243 % to 97.4 %), MR (97.4 % to 103.8 %), and UTR (103.8 % to 104.8311 %), respectively. It can be seen from the figure that there is a good correlation between simulated and theoretical calculated values of R_{max} for MR. Moreover, there is a good correlation between simulated and theoretical values of R_{max} for LTR and UTR, except at U/V ratios operating near the Tip. A discrepancy between simulated and theoretical values of R_{max} can be seen at U/V ratio of 95.944 % for LTR and at a U/V ratio of 104.83 % for UTR. As discussed in [15], this discrepancy is due to that fact that the simulation is for finite field radius and finite length and there are differences from the ideal case using Mathieu Stability diagram calculations since: (1) some ions, which are theoretically unstable, are transmitted in the simulation because of the slow increase in the ion trajectory envelope with distance along the QMF; (2) similarly, some ions, which are theoretically stable, are lost because the ion trajectory envelope is so high that they collide with the electrode if the QMF has finite field radius.

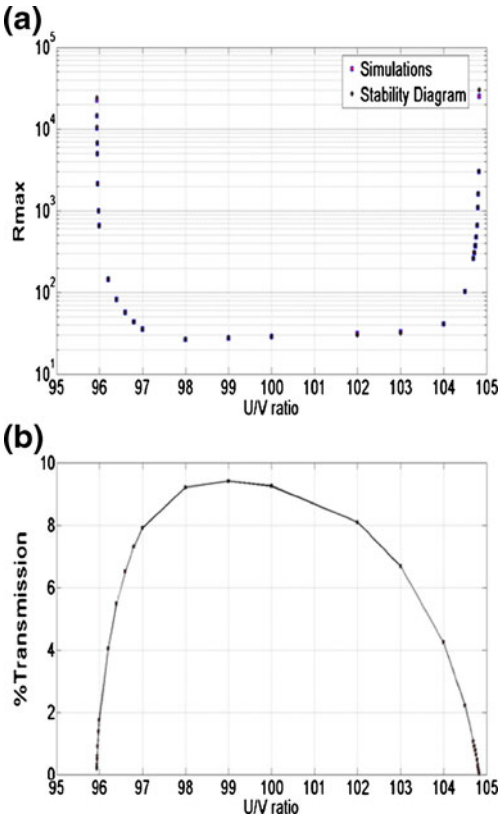

Figure 5. **(a)** Comparison of maximum resolution obtained in the simulations and the *Rmax* calculated for the ideal case using the Mathieu Stability diagram at different U/V ratios for LTR, MR and UTR; **(b)** the variation of percentage transmission with U/V ratio

However, in all cases, the trend observed is similar to the theoretical model (stability diagram), and only at high U/V ratios there is a discrepancy in the maximum resolution, since a slight change in Δq *or* Δa in simulations will change the resolution by a large amount. Figure 5b shows the variation of percentage transmission along the whole range of U/V ratios. It can be seen from Figure 5b that transmission is generally higher at the LTR compared with UTR of zone 3; thus LTR has better resolution versus transmission characteristics e.g., for an *Rmax* of 4938 at 95.95 % U/V, the percentage transmission is 0.58 %, whereas for a much smaller resolution 2985 at 104.82 % in the UTR, the percentage transmission is 0.12 %. Therefore, for a QMF operating in stability zone 3, the lower tip region has an advantage over the upper tip region in terms of transmission.

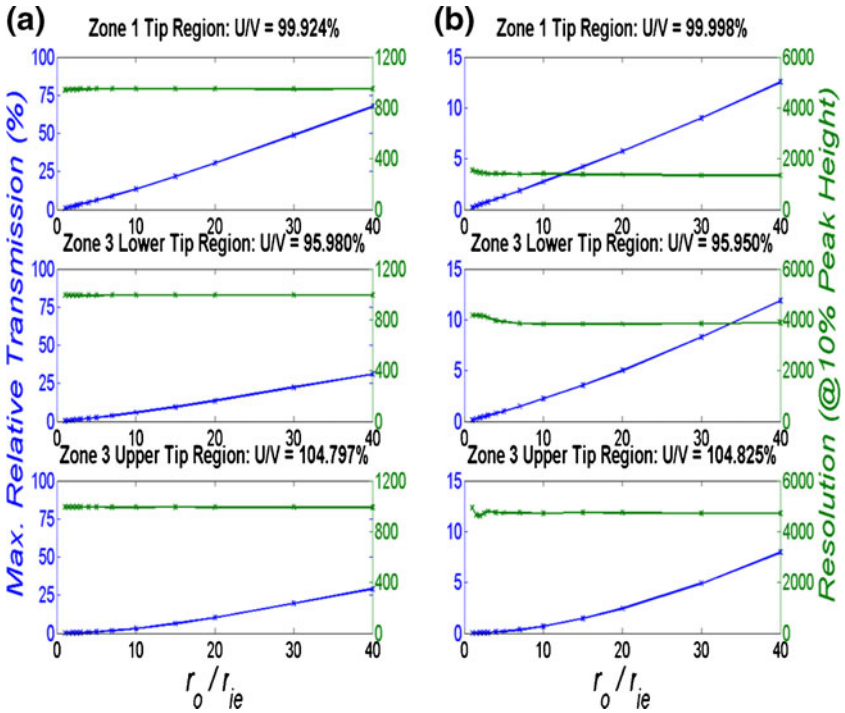

Figure 6. The variation of resolution and percentage transmission with r_0/r_{ie} ratio for zone 1, LTR of zone 3 and UTR of zone 3: **(a)** At U/V ratios proving an R_{max} of 1000, **(b)** randomly picked U/V ratios (L = 200 mm)

Resolution Versus Transmission Characteristics

Resolution versus transmission characteristics for QMF operation in stability zones 1 and 3 have been studied for different operating conditions. Figure 6a shows resolution (green line) versus percentage transmission (blue line) characteristics at different r_0/r_{ie} ratio for three different cases, stability zone 1, LTR of zone 3, UTR of zone 3. To get an appropriate comparison, the QMF is simulated at a saturated point of the performance curves and at a U/V ratio that gives an R_{max} of approximately 1000 for all the three different cases. As observed from Figure 6a, transmission increases linearly with increase in r_0/r_{ie} ratio for all the cases, but the increase is higher for stability zone 1. At $r_0/r_{ie} = 40$, the relative transmission for stability zone 1 is approximately 67.50 %, for zone 3 LTR it is 31.00 % and for zone 3 UTR it is 29.00 %. From these observations, and for this particular case, it can be said that zone 1 has better resolution versus transmission characteristics compared with stability zone 3. Also, it should be noted that zone 3 LTR has slightly better transmission than zone 3 UTR for same value of resolution.

Figure 6a tends to agree with the conventional belief [10, 14] that zone 3 suffers from a large amount of loss in transmission compared with zone 1. However, this is not always the case. Figure 6b shows resolution versus percentage transmission characteristics with increasing r_0/r_{ie} ratio for a QMF of length 200 mm (N = 168) for the same case as Figure 6a, but operated with U/V ratio close to the tip: 99.998 % for zone 1, 95.95 % for LTR of zone 3, and 104.825 % for UTR of zone 3, providing a resolution of 1339, 3875, and 4710, respectively. In all the three cases, zone 1, LTR of zone 3, and UTR of zone 3, transmission increases linearly with increase in r_0/r_{ie} ratio. Nevertheless, the increase at $r_0/r_{ie} = 40$ is quite low (7.90 %) for UTR of zone 3 compared with LTR of zone 3 (11.87 %) and stability zone 1(12.54 %). At $r_0/r_{ie} = 40$ from the results it is evident that even though there is a slight amount of loss in transmission from (12.54 % to 11.87 %) if the QMF is operated in LTR of zone 3 rather than zone 1, resolution is greatly enhanced by a factor of more than 2.5 (from 1339 to 3875). UTR of zone 3 has better resolution than both zone 1 and LTR of zone 3, but it suffers from considerable loss of transmission. It can be concluded from the case studied, as shown in Figure 6b, that LTR of stability zone 3 has the optimum resolution versus transmission characteristic.

Conclusions

The performance curve (i.e., the resolution (R) versus number (N) of radio frequency (rf) cycles experienced by the ions in the mass filter has been modeled for upper left tip and lower right tip of stability zone 3. The model has been used to accurately simulate performance curves published previously for operation in this stability zone. The saturation behavior of the performance curve observed in practice is seen to be the limiting feature of QMF performance and, therefore, not necessarily due to mechanical deficiencies. This is attributed to the fact that for a QMF, there is a finite theoretical limit to its resolution for a particular value of operating point (scan line),

since at that particular point Δq or Δa cannot go beyond a certain minimum value with any meaningful ion transmission. Furthermore, new design equations are established by examining the intersection of the scan line with stability zone 3. The maximum resolution $\boldsymbol{R_{max}}$ can also be related to stability parameter $\boldsymbol{a}$ as $\boldsymbol{R_{max} = a/\Delta a,}$ and R_{max} dependence on U/V ratio and stability parameters a and q are presented. According to the relationship given earlier with parameters shown in Table 1, the equations developed will be of importance to the QMS community in designing QMFs for operation in stability zone 3 and the electronics to drive them.

The Mathieu stability zone 3 can be divided into three regions of operation: lower tip region, middle region, and upper tip region. The lower tip region of zone 3 has better resolution versus transmission characteristics than the upper tip region. It has been previously published that transmission in zone 3 is consistently poorer than in zone 1. Whilst this is generally the case, our simulations indicate that for operation near the stability tip, zone 3 operation can deliver similar transmission as zone 1 but with superior resolution. The performance varies for zones 1 and 3 depending on the instrument operating parameters.

References

1. Paul, W., Raether, M.: Das elektrische massenfilter. *Z. Phys.* **40**, 262–273 (1955)
2. Brubaker, W.M., Tuul, J.: Performance studies of a quadrupole mass filter. *Rev. Sci. Instrum.* **35**(8), 1007–1010 (1964)
3. Taylor, S., Tunstall, J.J., Leck, J.H., Tindall, R.F., Jullien, J.P., Batey, J., Syms, R.R.A., Tate, T., Ahmad, M.M.: Performance improvements for a miniature quadrupole with a micromachined mass filter. *Vacuum* **53**, 203–206 (1999)
4. Ma, F.M., Taylor, S.: Simulation of ion trajectories through the mass filter of a quadrupole mass spectrometer. *IEE Proc-Sci. Meas. Technol.* **143**(1), 71–76 (1996)
5. Hiroki, S., Abe, T., Murakami, Y.: Separation of helium and deuterium peaks with a quadrupole mass spectrometer by using the second stability zone in the Mathieu diagram. *Rev. Sci. Instrum.* **63**(8), 83874–83876 (1992)
6. Hiroki, S., Abe, T., Murakami, Y.: Detection of a 10^{-4} helium peak in a deuterium atmosphere using a modified high-resolution quadrupole mass spectrometer. *Rev. Sci. Instrum.* **65**(6), 1912–1917 (1994)
7. Syed, S.U.A.H., Sreekumar, J., Gibson, J.R., Taylor, S.: QMS in the third stability zone with a transverse magnetic field applied. *J. Am. Soc. Mass Spectrom.* **22**, 1381–1387 (2011)
8. Douglas, D.J.: Linear quadrupoles in mass spectrometry. *Mass Spectrom. Rev.* **28**, 937–960 (2009)
9. Hogan, T.J., Taylor, S.: performance simulation of a quadrupole mass filter operating in the first and third stability zones. *IEEE* **57**(3), 498–508 (2008)
10. Du, Z., Douglas, D.J., Konenkov, N.: Elemental analysis with quadrupole mass filters operated in higher stability regions. *J. Anal. At. Spectrom.* **14**(8), 1111–1119 (1999)
11. Dawson, P.H.: Quadrupole Mass Spectrometry and Its Applications. Elsevier, Amsterdam (1976)
12. Paul, W., Reinhard, H.P., Von, Z.U.: Das elektrische massenfilter asl massenspektrometer and isotopentrenner. *Z. Phys.* **152**, 143–182 (1958)
13. Titov, V. V. Detailed study of the quadrupole mass analyzer operating within the first, second, and third (intermediate) stability regions. II. Transmission and resolution. *J. Am. Soc. Mass Spectrometry*. **9**, 70–87 (1998)
14. Konenkov, N.V., Kratenko, V.I.: Characteristics of a quadrupole mass filter in the separation mode of a few stability regions. *Int. J. Mass Spectrom. Ion Processes* **108**, 115–136 (1991)
15. Syed, S.U.A.H., Hogan, T.J., Gibson, J.R., Taylor, S.: Factors influencing the QMF resolution for operation in stability zones 1 and 3. *J. Am. Soc. Mass Spectrom* **23**, 988–995 (2012)
16. March, R.E., Todd, J.F.J.: Quadrupole Ion trap Mass Spectrometry. Wiley, New Jersey (2005)
17. Zhang, S.C., Jin, J.M.: Computations of Special Functions. Wiley, New York (1996)